X-ray Emission from the Radio Jet in 3C 120

Harris, D. E.; Hjorth, J.; Sadun, A. C.; Silverman, J. D.; Vestergaard, Marianne

Published in:
Astrophysical Journal

DOI:
10.1086/307284

Publication date:
1999

Accepted for publication in the ApJ; 1999 Jan 6
Preprint typeset using LaTeX style emulateapj

X-RAY EMISSION FROM THE RADIO JET IN 3C 120

D.E. Harris[1], J. Hjorth[2], A.C. Sadun[3], J.D. Silverman[4],
and
M. Vestergaard[1,2]

Accepted for publication in the ApJ; 1999 Jan 6

ABSTRACT

We report the discovery of X-ray emission from a radio knot at a projected distance of 25″ from the nucleus of the Seyfert galaxy, 3C 120. The data were obtained with the ROSAT High Resolution Imager (HRI). Optical upper limits for the knot preclude a simple power law extension of the radio spectrum and we calculate some of the physical parameters for thermal bremsstrahlung and synchrotron self-Compton models. We conclude that no simple model is consistent with the data but if the knot contains small regions with flat spectra, these could produce the observed X-rays (via synchrotron emission) without being detected at other wavebands.

Subject headings: galaxies: active—galaxies: individual (3C 120)—galaxies: jets—galaxies: Seyfert—radiation mechanisms: non-thermal—radio continuum: galaxies

1. INTRODUCTION

The emission process for the X-rays from knots and hotspots in extragalactic radio jets is generally thought to arise from one (or more) of three generally viable processes: thermal bremsstrahlung (TB), synchrotron self-Compton (SSC), and synchrotron emissions. Whilst quite convincing synchrotron and SSC models have been developed for particular sources (e.g. M87 [Biretta, Stern, & Harris 1991] and Cygnus A [Harris, Carilli, & Perley 1994]), TB models generally require a gas density sufficient to produce observable Faraday effects which are not seen. For other sources (e.g. Pictor A and 3C 273 [Röser, private communication]), none of these three processes is satisfactory.

Since only a handful of radio knots and hotspots have been detected in the X-ray band, more examples are continually sought to obtain additional constraints on the physical parameters implied for each type of model. For this reason, we proposed ROSAT HRI observations of 3C 120 when optical emission was reported for a segment of the inner radio jet (Hjorth et al. 1995). Our purpose was to see if we could detect the bright radio knot 4″ from the galactic nucleus, plus the following segment of the radio jet which was the section seen in the optical. Although our data were beset with problems which have made a detailed study of the area near the nucleus difficult, we find X-ray emission coincident with the relatively faint radio knot 25″ to the northwest of the nucleus (see Fig 1).

In this paper we give the essential X-ray parameters from our observation, briefly describe the processing techniques, discuss the astrometry, and consider the emission process responsible for the X-rays. 3C 120 is a Seyfert 1 radio galaxy at a redshift of 0.033. We use a Hubble constant of 50 km s^{-1} Mpc^{-1} which gives a distance of 200 Mpc and a scale of 0.91 kpc $arcsec^{-1}$.

2. OBSERVATIONS AND IMAGE PROCESSING

2.1. *The Data*

The observation consisted of two segments (hereafter "A" and "B"). Segment A was observed between 1996 August 16 and September 12 in 24 observation intervals ("OBIs") for a total live time of 37,036 s. Segment B was observed 1997 March 3-8 with 18 OBIs and 18,139 s. Segment A is seriously compromised by problems with the aspect determination of the satellite, resulting in an extended (east-west) tear-drop shape for the strong X-ray emission from the nucleus of the galaxy. A temporal analysis demonstrated this to be caused by an instrumental effect and since the nuclear X-ray emission is highly variable (Halpern 1985) most of the emission must be unresolved; our resolution is of order a few kpc whereas the apparent size of a source varying on a year timescale must be less than one pc. Segment B (Figure 1) was much better, with only mild broadening of the HRI Point Response Function (PRF). Because of these differences we analyzed the two segments separately.

2.2. *Ex post facto improvement of the effective PRF*

We have developed a method of improving HRI images which contain a strong source and which suffer from aspect problems ascribed to imperfections in the star tracker. These techniques are described in Harris et al. (1998a) and in that paper both segments of the 3C 120 observation were used as illustrative examples (see figs. 2 and 3 of Harris et al. 1998a). Since the primary aspect problem addressed is believed to be associated with the ROSAT 'wobbling' (a dither about the nominal pointing position with a period of 402 s), the term "dewobble" is used hereafter to describe the process of phase binning, centroiding, shifting, and restacking.

[1]CfA, 60 Garden St., Cambridge MA 02138; harris@cfa.harvard.edu, mvestergaard@head-cfa.harvard.edu
[2]Astronomical Observatory, University of Copenhagen, Juliane Maries Vej 30, DK-2100 Copenhagen, Denmark; jens@astro.ku.dk
[3]Department of Physics, University of Colorado at Denver, Campus Box 157, P.O. Box 173364, Denver, CO 80217-3364; asadun@carbon.cudenver.edu
[4]Dept. of Astronomy, University of Virginia, PO Box 3818, Charlottesville, VA 22903-0818; jds6h@ariel.astro.virginia.edu

2.3. *Astrometry for the X-ray emission from the 25″ radio knot*

The segment B X-ray map is superior to the longer exposure segment A since the effective PRF (even after dewobbling) is smaller and more circular. Therefore, except for intensity measurements, we confine our discussion to segment B. Absolute positions from the ROSAT aspect system are generally good to a few arcsec. We find an offset between the radio and X-ray cores of Δ RA = 0″.75 and Δ DEC = 2″.0 (Δ r = 2″.1). The overlays of the X-ray and radio maps in this paper always shift the X-ray map so as to align the nucleus with that of the radio.

The position of the X-ray knot relative to the nucleus is found to be 25″.7 in position angle -64.5°. To within the measuring errors (one arcsec and one degree) these values are the same as those for the peak radio brightness of the 25″ knot with respect to the radio core although the actual X-ray peak is a bit closer to the outer edge of the radio knot (see figure 2). With this precision afforded by the registration of the bright nucleus, and since there is no optical candidate (m_V > 19 mag.) for the X-ray emission, we are convinced that the area containing the peak radio brightness and outer edge of the 25″ knot is the correct identification for the X-ray emission.

3. X-RAY PARAMETERS OF THE 25″ KNOT

As a check on our methods of intensity measurement we derived the countrate and flux for the nuclear emission which is known to be highly variable at X-ray and other wavelengths (Halpern 1985). To compare the current X-ray values with those of Halpern we measured the counts with an aperture of r=19″ (at the radius of the brightness minimum between the nucleus and the 25″ knot; see figure 1). For the conversion from counts/s to flux, we assumed a spectral model consistent with the findings of Halpern: the galactic value of neutral hydrogen (log NH = 21.035) and a power law with energy index 0.7. Our resulting flux values for the 2 to 10 keV band (segment A: 6.66×10^{-11} ergs s^{-1} cm^{-2}; segment B: 6.10×10^{-11} ergs s^{-1} cm^{-2}, with statistical uncertainties of less than one percent for both values) are slightly greater than the range of 2 to 5×10^{-11} erg s^{-1} cm^{-2} found by Halpern in 1980 with the Einstein MPC.

The spatial geometry chosen to measure the intensity of the knot is designed to minimize the effects of the wings of the PRF from the strong nuclear emission and is based on a contour diagram of the smoothed (FWHM=3″) segment B image. Even though the knot is not well defined in segment A, the same geometry was applied. We defined an annulus centered on the nucleus with inner and outer radii of 19″.5 and 31″.5 respectively. The segment of this annulus between PA = 280° and 310° contains the X-ray knot. The inner radius of the annulus was chosen to lie at the saddle point in X-ray brightness (between the core and the knot distributions), and the overall size in both dimensions is close to 12″. Thus we used the r=6″ scattering correction (1.26; David et al. 1995). The background brightness was estimated from the remainder of the same annulus, except for segment A where the pie section (30° wide) south of the knot was rejected since it contained residual nuclear emission.

We measured both the original data and the dewobbled version. For segment B there was excellent agreement between the two versions, whereas for segment A it was clear that the original map should not be used because of the instrumental spreading of the nuclear emission. The results are given in Table 1. From the measured countrates, there is no evidence for X-ray variability of the knot. The FWHM of a Gaussian fit to the 3″ smoothed map of the knot is 7″.6 × 6″.0, slightly smaller than the X-ray size of the nuclear emission, but entirely consistent with the core size given the small number of counts defining the knot. Thus the X-ray knot is unresolved.

4. DISCUSSION

4.1. *Spectrum*

Radio flux densities were measured from VLA maps kindly supplied by R. C. Walker (the same data used in Walker et al. 1987). All the radio maps (1.4, 5, and 14.9 GHz) were constructed to have the same beam size of 1″.25. We used two rectangles to measure flux densities; one which included the whole knot and the other which isolated the outer edge and peak of the knot. The results are given in Table 2.

The optical (B and I bands) upper limits were obtained with a circular aperture of diameter 4″ from the same data used in Hjorth et al. (1995). The measurements were corrected for galactic extinction and are given in Table 3.

The spectrum of the knot is plotted in Figure 3. From the optical upper limits, it is clear that a single power law fit from the radio data to the X-ray point is precluded.

4.2. *A Thermal Model*

The difficulties generally encountered in applying a TB model to radio hotspots are twofold. The first problem is how to maintain an over-pressured mass of hot gas outside a galaxy. To explain the observed X-ray emission with a TB model, a mass of some 10^9 $M_\odot$ at a temperature of order several 10^6 K is required in a volume characterized by a radius of a few kpc. The resulting pressures usually exceed those expected in the IGM by factors significantly greater than one. The second problem is that no anomalous Faraday effects are observed in the radio polarization studies, and with only small values of the presumed magnetic field, both depolarization and anomalous Faraday rotation would be expected from the purported hot gas (e.g. Cygnus A [Harris et al. 1994]; M87 [Biretta et al. 1991] ; 3C 390.3 [Harris, Leighly, & Leahy 1998b]).

For the 3C 120 knot, a uniform sphere of gas with a radius of 3″ (2.7 kpc) would have the parameters listed in Table 4 in order to produce the observed X-ray intensity. Since the 25″ knot is located at least 23 kpc from the center of the galaxy, we think the thermal model entails improbable conditions for the maintenance of the required over-dense gas as a discernible entity. Furthermore, Walker et al. (1987) state that "Any Faraday rotation or depolarization is too small to be detected in these observations." A thermal model for the X-ray emission would most likely produce observable polarization effects since the rotation measure for a pathlength of 5.4 kpc with even a small magnetic field like 10 μG would be ≈9000 radians m^{-2} (Walker et al. find upper limits of ≈50 rad m^{-2}). Thus, to sustain a TB model, the gas would have to be behind the radio knot and aligned with it by chance when viewed from the Earth.

4.3. *An SSC Model*

SSC emission is the process of choice for the radio hotspots of Cygnus A (Harris et al. 1994). In that case, the average magnetic field strength required for the SSC model is entirely consistent with the value found from the radio data alone under the classical assumption of minimum energy conditions. However, for the other known examples of X-ray emission from radio hotspots, the SSC model fails because the observed radio brightness is much too small to provide the required photon densities. This is true also for 3C 120. We estimate the photon energy density by extending the radio spectrum from 10^7 to 10^{14} Hz with a power law of $\alpha = 0.65$ (Walker et al. 1987). For an emitting volume of a cylinder corresponding to the deconvolved FWHM of the 6 cm radio map (r=0.″25, length=1.″23) the resulting photon energy density is 2×10^{-13} erg cm^{-3} and the ratio of inverse Compton to synchrotron emissions would be 0.004 (B $\approx$40 μG). The predicted SSC flux density at 2 keV is more than 4 orders of magnitude less than that observed.

4.4. *A Synchrotron Model*

Synchrotron models require relativistic electrons with Lorentz energy factors of 10^7 in typical magnetic fields of order 100 μG. For the case of knot A in the M87 jet, the synchrotron model for the X-ray emission is preferred because the optical jet is almost certainly caused by synchrotron emission, and the steepening of the power law spectra in the optical, when extrapolated to the X-ray band, are in reasonable accord with the observed X-ray intensity (Biretta et al. 1991). 3C 390.3 (hotspot B) is another case for which the synchrotron model appears to be favored (Harris et al. 1998b).

To get synchrotron X-ray emission from the brightest part of the radio knot requires electrons with Lorentz energy factors of 4×10^7 for a magnetic field strength of 40 μG (the equipartition value). These electrons would have a synchrotron halflife of 132 years. Our optical upper limits (figure 3) mean that the power law connecting the radio and X-ray flux densities is not an acceptable spectrum unless more than 2.4 mag of excess absorption is present in the B band (more than 1.5 mag in the I band). Note that these excesses refer to a line of sight which passes no closer than 22 kpc to the nucleus and there is a high probability that the 25″ knot is closer to us than the galaxy because the inner segment of the jet shows beaming effects. For a synchrotron model with the usual power law distribution of relativistic electrons, it would be necessary to hypothesize the presence of a flat spectrum component ($\alpha \leq 0.4$) such that the optical flux densities would lie below the observed upper limits and the radio flux densities would be too weak to be isolated from the surrounding emission.

Physically, such a feature might be a localized volume within the knot where the shock structure is such as to extend the electron spectrum to the higher energies required to produce X-ray synchrotron emission. Kirk (1997) discusses how mildly relativistic shocks and oblique magnetic fields can produce particle energy distributions with power law spectra flatter than the canonical distribution from non-relativistic shocks.

In Table 5 we give the synchrotron model requirements for four possible volumes. These parameters are reasonable for a small region within the radio knot although the actual magnetic field values might be governed by larger scale structures and thus differ from the particular entries. Although for most stationary non-thermal sources, E^2 losses steepen the particle distribution at the higher energies, the synchrotron halflives given in Table 5 are sufficiently long that this effect is not required for transient phenomena. The canonical spectral steepening comes about for a constant injection spectrum operating over times much longer than the loss time-scale at the highest energies. We envisage a process that arises from time to time at various locations in the knot but that is not a single, long lasting feature.

If these small regions are the correct explanation for the X-ray emission from the 3C 120 knot, they might be present also in other sources. The observed decrease of X-ray intensity in knot A of the M87 jet led Harris, Biretta, & Junor (1997) to suggest that the X-ray structure of knot A would be smaller than that in the radio and optical. The combined spectral and spatial resolutions of AXAF are well suited to test our hypothesis.

5. SUMMARY

With the possible exception of 3C 273, the one common characteristic found for radio jet features which emit observable X-rays is a strong gradient in the radio brightness. For M87 knot A, this is the edge facing up stream, toward the nucleus. For 3C 390.3 it is the outer edge of hotspot B where the jet appears to impinge on a dwarf galaxy which is a member of the 3C 390.3 group. In the case of 3C 120, the observed X-ray location is also the site of a strong gradient in radio brightness. Given the normal interpretation of these features as indications of a strong shock front, a synchrotron explanation of the X-ray emission remains the most likely possibility even if it necessitates the existence of one or more hitherto unnoticed components.

We thank Craig Walker for supplying us with his radio maps of 3C 120 and H. Falcke, the referee, for useful comments which led to improvements in the paper. Work at the SAO was partially supported by NASA contract NAS5-30934 and NASA grant NAG5-2960.

REFERENCES

Biretta, J. A., Stern, C. P., & Harris, D. E. 1991, AJ 101, 1632
David, L. D. et al. 1995, "The ROSAT High Resolution Imager", a.k.a. "The HRI Calibration Report", a document which undergoes occasional revisions, available from URL http://hea-www.harvard.edu/ROSAT/rsdc_www.hricalrep.html.
Halpern, J. P. 1985, ApJ 290, 130
Harris, D. E., Carilli, C. L. & Perley, R. A. 1994, Nature 367, 713
Harris, D. E., Biretta, J. A., & Junor, W. 1997, MNRAS 284, L21
Harris, D. E., Leighly, K. M., & Leahy, J. P. 1998b, ApJ 499, L149
Harris, D. E., Silverman, J. D., Hasinger, G., & Lehmann, I. 1998a, A&AS (scheduled for 1 Dec. 98).
Hjorth, J., Vestergaard, M., Sørensen, A. N., & Grundahl, F. 1995, ApJ 452, L17
Kirk, J. G. 1997, in Relativistic Jets in AGNs, ed. M. Ostrowski et al. (Cracow: Poligrafia Inspektoratu Towarzystwa Salezjańskiego), 145 (or see astro-ph/9708040)
Walker, R. C., Benson, J. M., & Unwin, S. C. 1987, ApJ 316, 546
Walker, R. C. 1997, ApJ 488, 675

Fig. 1.— An overlay of the X-ray and radio maps. The 5 GHz radio map was provided by R. C. Walker from VLA observations (see Walker, 1997). The X-ray map has been smoothed with a Gaussian of FWHM = $3''$, and the peak intensity has been aligned with the radio peak. In units of 0.15 counts/pixel (pixels are $0''.5$), the contour levels are drawn at 1, 2, 3, 4, 6, 8, 10, 15, 20, 25, 50, 75, 100, and 200.

Fig. 2.— The $25''$ knot. Only segment B of the observations is used for the X-rays (greyscale). The radio map was provided by R. C. Walker from VLA observations (see Walker, 1997). In units of 30 μJy/beam, the contour levels are $\pm$1, 2, 3, ... 10, 12, 14, ... 20. The restoring beam size is $0''.365$.

Fig. 3.— The spectrum of the $25''$ knot. For the radio data, we used the values measured with the smaller box centered on the bright peak (Table 2). The X-ray point is from Table 1 and the optical upper limits from Table 3.

Table 1

X-ray intensity measurements of the $25''$ knot

Observation	Net Counts	Countrate (counts ks^{-1})	Flux (0.2-2keV) (erg cm^{-2} s^{-1})	S(2keV) (μJy)	Lx(0.2-2keV) (ergs s^{-1})
segment A	74.6$\pm$14	2.5 (19%)	1.50×10^{-13}	0.018	7.16×10^{41}
segment B	35.5$\pm$7.2	2.5 (20%)	1.45×10^{-13}	0.017	6.95×10^{41}

Note.—The countrate column includes the appropriate scattering correction of 1.26 and the indicated percentage errors (one sigma) apply also to the following columns. The flux column gives the so called “unabsorbed” flux which, for the chosen spectral model, is 1.8 times larger than the observed flux. For the (unabsorbed) flux density (S) a μJy is equivalent to 10^{-29} ergs cm^{-2} s^{-1} Hz^{-1}. The spectral model used to convert count rate to flux and luminosity includes the galactic absorption (log NH = 21.035) and a power law with energy index α=0.7 (the power law which connects the radio and the X-ray data). For other spectral models, the reader can consult the behavior of the relevant conversion factors given in David et al. (1995).

TABLE 2
RADIO FLUX DENSITIES OF THE 25″ KNOT

Frequency (GHz)	S(total) (mJy)	S(partial) (mJy)	Peak(partial) (mJy/beam)
1.452	30.8	17.4	6.86
4.985	16.8	9.2	3.41
14.915	4.5	2.9	1.42

NOTE.—The rectangle used for the total flux density of the knot was 7.″2× 6.″6. For the peak brightness and outer edge (designated "partial"), the box was 3.″6×4.″5.

Table 3. Upper Limits for the Optical Flux Densities

log Frequency (Hz)	S (μJy)
14.52	$\leq$0.707
14.834	$\leq$0.181

TABLE 4
THERMAL BREMSSTRAHLUNG MODEL PARAMETERS

kT (keV)	Unabsorbed Flux (erg cm^{-2} s^{-1})	Density (cm^{-3})	Pressure (dyne cm^{-2})	Mass (M$_\odot$)
1	1.56×10^{-13}	0.23	7.1×10^{-10}	4.9×10^{8}
3	1.33×10^{-13}	0.21	1.9×10^{-9}	4.3×10^{8}
6	1.29×10^{-13}	0.22	4.0×10^{-9}	4.6×10^{8}

NOTE.—The calculations were performed on the basis of a uniform density gas filling a sphere of radius 2.7 kpc (consistent with the HRI PRF for an unresolved source). For smaller radii the density and pressure increase whereas the total mass decreases. The flux listed is for the 0.2 to 2 keV band.

Table 5
Synchrotron Parameters for Flat Spectrum Components

Radius (arcsec)	Radius (pc)	B(min) (μG)	P(min) (dynes cm^{-2})	log E(tot) (ergs)	γ_X	τ (yrs)
0.5	450	9	8×10^{-12}	53.27	1.1×10^{8}	750
0.1	91	38	1×10^{-10}	52.37	5.5×10^{7}	100
0.05	45	70	4×10^{-10}	52.05	4.1×10^{7}	42
0.01	9	277	7×10^{-9}	51.15	2.0×10^{7}	5

Note.—The basic spectrum is constructed from the observed X-ray flux density with α=0.4 and frequency limits of 100 MHz and 4.8×10^{17} Hz (2keV). The total energy is that stored in relativistic particles and magnetic fields. γ_X is the Lorentz energy factor of the electrons responsible for the 2 keV emission and τ is the synchrotron half-life of those electrons.

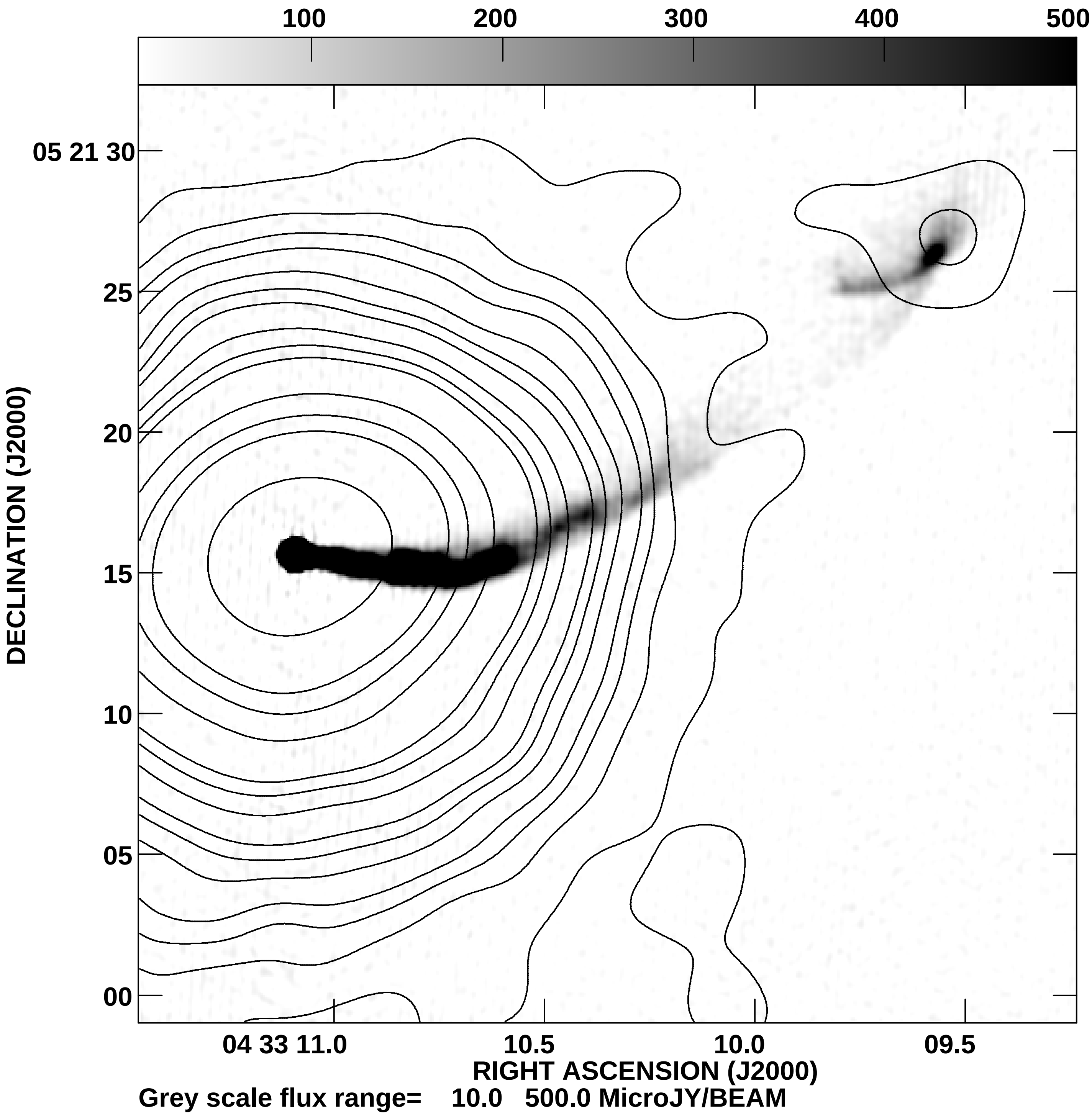

100
200
300
400
500
05 21 30
25
20
15
10
05
00
DECLINATION (J2000)
04 33 11.0
10.5
10.0
09.5
RIGHT ASCENSION (J2000)
Grey scale flux range= 10.0 500.0 MicroJY/BEAM

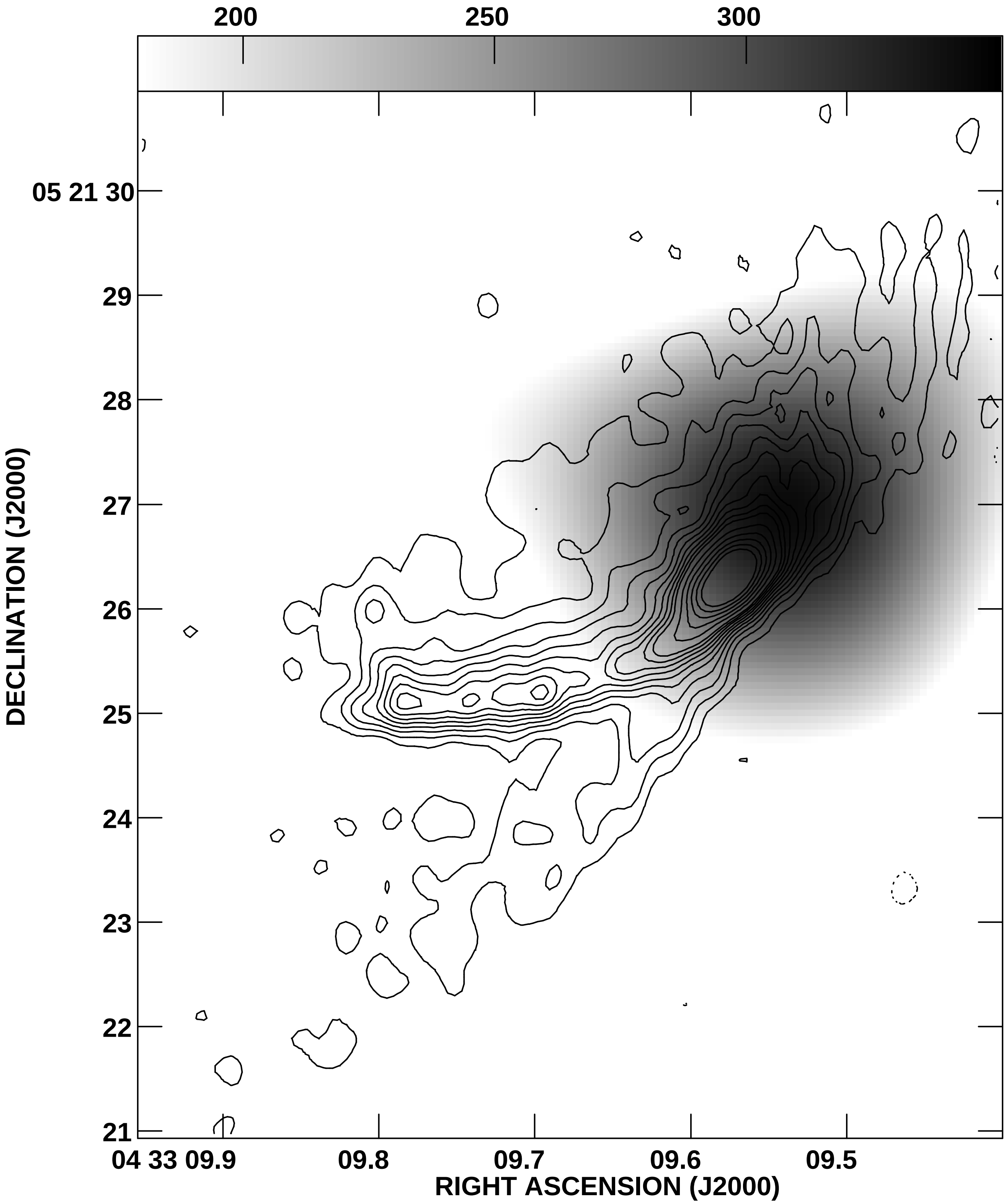

200
250
300
05 21 30
29
28
27
26
25
24
23
22
21
DECLINATION (J2000)
04 33 09.9
09.8
09.7
09.6
09.5
RIGHT ASCENSION (J2000)

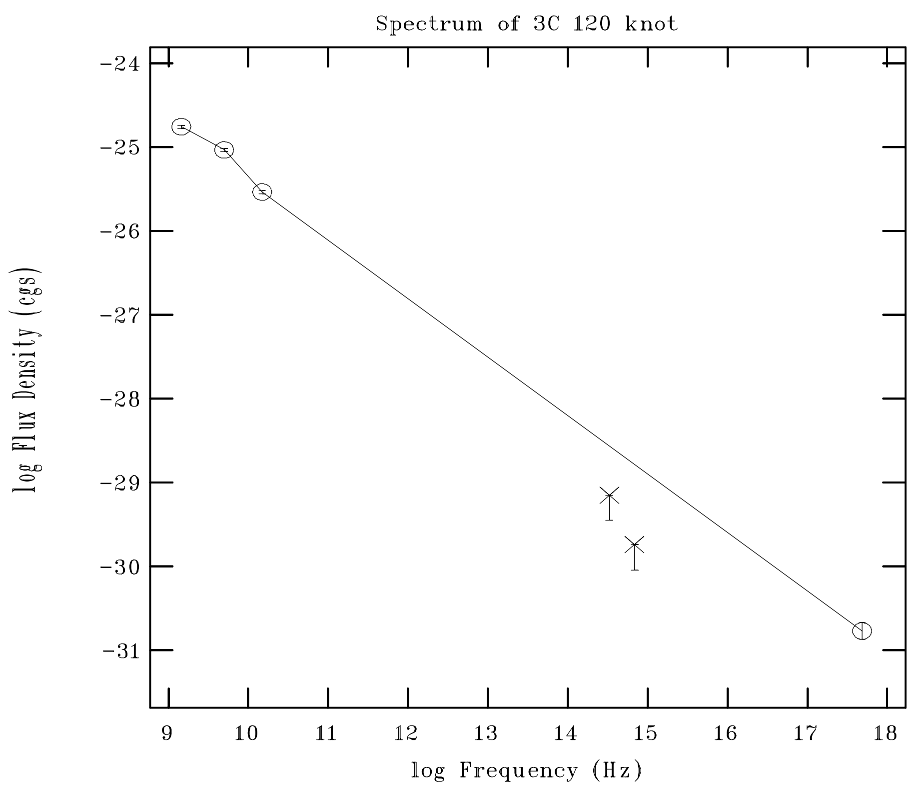
Spectrum of 3C 120 knot
log Flux Density (cgs)
log Frequency (Hz)
-24
-25
-26
-27
-28
-29
-30
-31
9
10
11
12
13
14
15
16
17
18